





Reconstructing rare particle source by femtosopic correlations

Liang Zhang(张良) ^{1,2}, Song Zhang(张松) ^{1,3,*}, Kai-Jia Sun(孙开佳) ^{1,3,†} and Yu-Gang Ma(马余刚) ^{1,3,4,‡}

¹*Key Laboratory of Nuclear Physics and Ion-beam Application (MOE), Institute of Modern Physics, Fudan University, Shanghai 200433, China*

²*Shanghai Institute of Applied Physics (SINAP), Shanghai, China*

³*Shanghai Research Center for Theoretical Nuclear Physics, NSFC and Fudan University, Shanghai 200438, China*

⁴*School of Physics, East China Normal University, Shanghai 200241, China*

Measurement of particle emission source is a fundamental objective of femtoscopy in high-energy nuclear collisions. Conventional analyses rely on Gaussian parameterizations of pair emission sources, which makes the extraction of single-particle emission sources challenging, particularly for rare particles. Here, we introduce a novel Statistical Reconstruction method that allows extracting information of target single-particle sources relative to a data-constrained reference source instead of the Gaussian assumption. The correlation function is expressed as an ensemble average over single-particle-conditioned correlation kernel, defined as the particle-by-particle contribution to the correlation function conditioned by the target particles. For particles with rare yields, the particle-by-particle distribution of this kernel can be transformed into event-by-event extraction and becomes experimentally accessible, enabling a direct statistical reconstruction of the single-particle emission source, instead of inferring a pair source. We apply this method to reconstruct J/ψ source via $p - J/\psi$ correlations, using HAL QCD-derived NJ/ψ potentials in $\sqrt{s} = 13.6$ TeV pp collisions simulated with EPOS4HQ. The reconstructed source reproduces the key characteristics and this new approach achieves a systematic uncertainty of approximately 13% based on EPOS4 simulation.

I. INTRODUCTION

Hanbury Brown and Twiss (HBT) first pioneered identical-particle intensity interferometry to measure the apparent angular diameter of remote stars [1]. In the 1960s, this concept was extended to high-energy physics [2], where HBT interferometry has since developed into a powerful tool for exploring the femtometer-scale spatio-temporal structure of particle-emission sources [3, 4] in intermediate-energy [5, 6] and high-energy [7–9] heavy-ion collisions, where provides an ideal venue to study properties of nuclear matter [10–15].

At such microscopic scales, correlation analyses must account for final-state interactions (FSI). This inclusion allows the method to be extended to non-identical particle pairs [16–24]. In the context of relativistic heavy-ion collisions, this methodology is commonly referred to as “femtoscopy” [7–9, 20, 21]. It is widely employed to characterize the geometry of emission sources [4, 17, 25–32] and dynamics of system evolution [33–38], and, more recently, to probe the nature of hadronic interactions at low relative momenta [16, 39–44], including studies of exotic hadrons and hadronic resonant states [11, 45–52].

The experimental measurements from the ALICE Collaboration has demonstrated that the emission sources of π , K , p and Λ in 13 TeV pp collisions at the LHC originate from a common hadron-emission source [27, 28].

These findings naturally raise the question of whether the emission sources of short-lived charm hadrons exhibit a similar spatial structure. Since charm hadrons are mainly produced at the early stage of the collision, their emission sources are expected to be more compact than those of longer-lived particles mentioned above. More fundamentally, conventional femtoscopy accesses source information only through two-particle observables, such that the single-particle emission source of charm hadrons is not directly measurable. As these hadrons are emitted during a non-equilibrium state, the commonly adopted Gaussian parameterizations should not be assumed a priori. Consequently, the extraction of charm-hadron emission sources within the standard femtoscopy framework remains an open problem.

With the continuous improvement of experimental precision, particle source extraction in femtoscopy has moved beyond traditional Gaussian parametrizations [4, 7, 25]. Since the particle emission source is inferred from measured two-particle correlation functions, source reconstruction constitutes an ill-posed inverse problem, motivating the development of various inverse approaches, including machine learning techniques [31], optical deblurring algorithms [29], and regularization methods such as Tikhonov regularization [30]. While these methods significantly improve the reconstruction of femtosopic sources, they are all formulated at the level of two-particle (pair) sources that are directly accessible through correlation measurements. In contrast, the direct extraction of a single-particle source, especially for rare particles, remains an open problem, as the single-particle emission information is implicitly folded into pair observables.

* song_zhang@fudan.edu.cn

† kjsun@fudan.edu.cn

‡ mayugang@fudan.edu.cn

In the present study, we introduce a Statistical Reconstruction method, which reformulates femtoscopy as an inverse problem for single-particle emission sources. The method is based on expressing the measured two-particle correlation as an ensemble average over single-particle-conditioned correlation kernels, whose distribution encodes the underlying target single-particle source. This reconstruction cannot be achieved within conventional source imaging approaches, which invert only the two-particle source. In practice, the reconstruction requires (i) a well-characterized emission source of an abundant reference hadron (e.g., pions or protons) which can be obtained by phenomenological models, and (ii) a constrained interaction potential, provided by effective field theories or lattice QCD.

As a proof of concept, we demonstrate the method through EPOS4HQ simulations [53–58], where the J/ψ emission source is reconstructed via p - J/ψ correlations with NJ/ψ potentials derived from HAL QCD calculations [59]. In this work, we focus on validating the stability and statistical uncertainty of the reconstruction method under controlled input conditions.

This paper is structured as follows. Sec. II introduces our Statistical Reconstruction method. Sec. III shows the reconstruction of the J/ψ source in EPOS4HQ simulation to validate the method. Finally, a summary is provided in Sec. IV.

II. STATISTICAL RECONSTRUCTION METHOD

A. Methodology

The two-particle momentum correlation function constitutes the fundamental observable in femtoscopy. It is defined as [7]

$$C(\mathbf{k}^*) = \int d^3\mathbf{r}_1 d^3\mathbf{r}_2 S_1(\mathbf{r}_1) S_2(\mathbf{r}_2) |\psi_{\mathbf{k}^*}(\mathbf{r}_1 - \mathbf{r}_2)|^2, \quad (1)$$

where $\mathbf{k}^* = \frac{1}{2}(\mathbf{p}_1 - \mathbf{p}_2)$ denotes the relative momentum in the pair rest frame, and \mathbf{r}_i the particle coordinates. $S_1(\mathbf{r}_1)$ and $S_2(\mathbf{r}_2)$ denote the normalized single-particle emission sources, while the $|\psi_{\mathbf{k}^*}(\mathbf{r}_1 - \mathbf{r}_2)|^2$ incorporates contributions from QS (for identical particles) and FSI. This formalism provides the basis for extracting source properties from experimental data, allowing a quantitative investigation of the space-time structure of particle-emitting sources.

In conventional approaches, particle emission sources are typically modeled as Gaussian distributions [4, 25, 41–43]. Recently, the ALICE collaboration proposed the Resonance Source Model (RSM) [27, 28], which incorporates a universal Gaussian core for primordially produced particles, along with an exponential tail from resonance-decay contributions. The two-particle Gaussian source

can be expressed as:

$$S_{12}(r) = \frac{1}{(4\pi R^2)^{3/2}} \exp\left(-\frac{r^2}{4R^2}\right). \quad (2)$$

This Gaussian parametrization continues to be widely adopted in femtoscopic analyses [28, 39, 43, 60, 61]. Motivated by these developments, it is necessary to test the universality of the Gaussian source for early-stage produced particles. In particular, one can investigate the J/ψ emission source via p - J/ψ correlations without assuming a Gaussian form.

Building on the conventional approach, two-particle source distributions are often inferred by fitting correlation functions with predetermined interaction wavefunctions. To isolate the source distribution of an individual particle, $S_1(\mathbf{r}_1)$, in Eq. (1), the integral can be rewritten as

$$C(k^*) = \int d\mathbf{r}_1 S_1(\mathbf{r}_1) \tilde{C}_{k^*}(\mathbf{r}_1), \quad (3)$$

where $\tilde{C}_{k^*}(\mathbf{r}_1)$, termed the single-particle-conditioned correlation kernel, represents the correlation between particle 1 located at r_1 and the ensemble of particle 2:

$$\tilde{C}_{k^*}(\mathbf{r}_1) = \int d^3\mathbf{r}_2 S_2(\mathbf{r}_2) |\psi_{k^*}(\mathbf{r}_1 - \mathbf{r}_2)|^2, \quad (4)$$

under the assumption of isotropic emission. For simplicity, the angular distribution of the source is taken to be uniform, and hereafter the angular-averaged source is denoted simply as $S_i(r_i)$.

Eq. (3) can be interpreted statistically, which corresponds to the mean value $\langle \tilde{C}_{k^*}(r_1) \rangle$ over a set of samples drawn from $r_1 \sim S_1(r_1)$. The probability of $y = \tilde{C}_{k^*}(r_1)$ can then be expressed as

$$p_{\tilde{C}_{k^*}}(y) = \int S_1(r) \delta(y - \tilde{C}_{k^*}(r)) dr, \quad (5)$$

which describes the transformation of the source distribution $S_1(r)$ into the distribution of y through the functional map $\tilde{C}_{k^*}(r)$. This property is essential, as it enables a direct statistical reconstruction of the single-particle emission source, rather than an indirect inference of an effective two-particle source. It should be noted that the extracted S_1 is not a distribution in absolute spacetime, but a relative distribution obtained after averaging the spatial distribution of particle 2. However, it still contains spatial information about particle 1.

Reversal of the thought of Eq. (5), a reconstruction strategy for source is presented as,

$$\begin{aligned} S_1^{(k^*)}(r) &= \int p(y) \delta\left(r - \tilde{C}_{k^*}^{-1}(y)\right) dy \\ &= \sum_j \left(p(y_j) \left| \tilde{C}'_{k^*}(r) \right| \right)_{y_j = \tilde{C}_{k^*}(r)}. \end{aligned} \quad (6)$$

Due to the potentially non-monotonicity of $\tilde{C}_{k^*}(r)$ function, the reconstructed source distribution $S_1^{(k^*)}(r)$ at individual k^* may deviate from original source distribution $S_1(r)$. In the following, we show that a coherent combination of reconstructions over multiple relative-momentum bins provides a robust estimate of the underlying source.

This approach fundamentally relies on two essential requirements, the distribution of $y = \tilde{C}_{k^*}(r_1)$ and the analytical calculation of $\tilde{C}_{k^*}(r)$. The latter one is based on the established inputs, a known single-particle source and a well-constrained interaction potential, as introduced in Sec. I.

In experiments, the correlation function $C(k^*)$ is determined through the normalized ratio [7, 27, 28]

$$C(k^*) = \mathcal{N} \frac{N^{\text{same}}(k^*)}{N^{\text{mixed}}(k^*)}, \quad (7)$$

where \mathcal{N} is the normalization factor, $N^{\text{mixed}}(k^*)$ represents the distribution of uncorrelated pairs obtained from event mixing, and $N^{\text{same}}(k^*) = \sum_i^{N_{\text{events}}} \sum_j^{N_T^i} n_{ij}^{\text{same}}(k^*)$ is the distribution of correlated pairs from the same event. Here N_{events} denotes the total number of events, N_T^i is the number of target particle to be reconstructed in i -th event and $n_{ij}^{\text{same}}(k^*)$ represents the pair number with momentum k^* including j -th target particle in i -th event. The corresponding conditioned kernel \tilde{C}_{k^*} for a target particle in the i -th event can then be defined as:

$$\tilde{C}_{k^*;ij} = \mathcal{N} N_T^{\text{tot}} \frac{n_{ij}^{\text{same}}(k^*)}{N^{\text{mixed}}(k^*)}. \quad (8)$$

This definition allows the particle-by-particle distribution of $y = \tilde{C}_{k^*}$ to be directly accessed experimentally, providing the statistical input required for reconstructing the single-particle emission source. However, experimentally determining the conditioned kernels challenging because it is difficult to isolate individual particles for pairing in a given event. Eq. 8 also incorporates particle production fluctuations into the kernel fluctuations, which increases the systemic uncertainty.

B. Validation

To validate the feasibility of our Statistical Reconstruction method, we perform a controlled numerical test. We use predefined Gaussian emission sources with radii $R_1 = 0.5$ fm and $R_2 = 1.4$ fm, and adopt the wave function

$$\psi_{\mathbf{k}^*}(\mathbf{r}) = \sqrt{2} \cos(\mathbf{k}^* \cdot \mathbf{r}). \quad (9)$$

The corresponding analytical correlation function is shown in Fig. 1. We then quantitatively evaluate the reconstruction accuracy by comparing the extracted source profiles against ground-truth inputs.

The validation initiates by sampling radial coordinates r_1 for particle 1 from source distribution S_1 . For

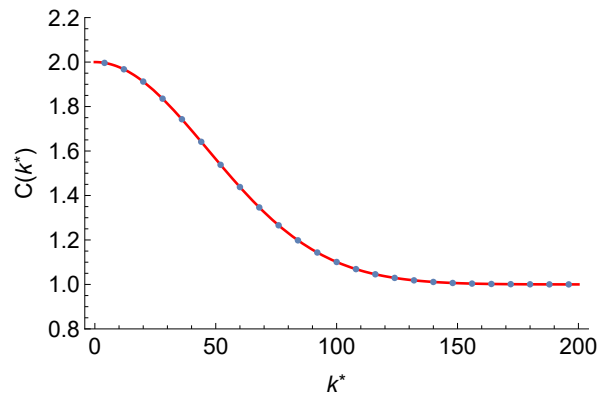


FIG. 1: The analytically computed correlation function derived from Gaussian emission sources with radii $R_1 = 0.5$ fm and $R_2 = 1.4$ fm, employs the wavefunction $\psi_{\mathbf{k}^*}(\mathbf{r}) = \sqrt{2} \cos(\mathbf{k}^* \cdot \mathbf{r})$. Blue markers denote candidate momenta selected for reconstruction validation.

each sampled coordinate, the $\tilde{C}_{k^*}(r)$, defined in Eq. (4), is evaluated over the range $r \in [0, 15]$ fm. The resulting distribution of $y = \tilde{C}_{k^*}(r)$ at $k^* = 100$ MeV is shown as a histogram in Fig. 2a.

The analytically form of $\tilde{C}_{k^*}(r)$, shown as the blue curve in Fig. 2b, is discretized on a 2D grid with 200 bins in y and 60 bins in r . Within each bin, the local slope $d\tilde{C}_{k^*}(r)/dr$ is calculated. These slopes are used to construct the reconstruction kernel K_{k^*} , where the elements $(K_{k^*})_{ij}$ are set to zero if the curve of $\tilde{C}_{k^*}(r)$ does not pass through the bin (r_i, y_j) .

To address regions where $\tilde{C}_{k^*}(r)$ varies rapidly and passes through multiple y -bins within a single r -bin, we implement a multiplicity-averaging procedure:

$$K_{ij} \rightarrow (K_{k^*})_{ij} / n_i^{\text{cross } y\text{-bins}}, \quad (10)$$

where $n_i^{\text{cross } y\text{-bins}}$ counts the number of y -bins traversed by the curve within the i -th r -bin. This prevents over-counting of probability when the reconstruction mapping is multi-valued.

The reconstructed source distribution at a given k^* is then obtained via,

$$S_1^{(k^*)}(r_i) = \frac{K_{k^*} \cdot \mathbf{y}^{\text{counts}}}{\sum_j y_j^{\text{counts}}} \Delta r_i, \quad (11)$$

where $\mathbf{y}^{\text{counts}}$ denotes the histogram-count vector of $\tilde{C}_{k^*}(r)$. As demonstrated in Fig. 2c, the reconstructed distribution agrees excellently with the ground-truth source.

However, not every reconstruction yields a success story. The non-monotonic behavior of $\tilde{C}_{k^*}(r)$ (Fig. 3) violates the bijectivity of reconstruction mapping. As a result, the reconstructed source distributions exhibit pronounced artifacts. For example, at $k^* = 156$ MeV (Fig. 4), spurious peaks arise in reconstruction because $\tilde{C}_{k^*}(r)$ processes non-zero slopes within $r < 3$ fm (Fig. 3b).

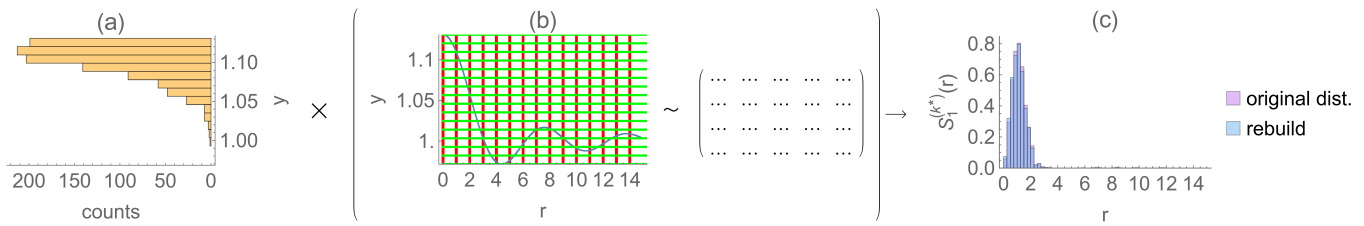


FIG. 2: Flowchart on reconstructing $S_1^{(k^*)}(r)$. Figure a shows the histogram of $y = \tilde{C}_{k^*}(r)$ where $k^* = 100$ MeV. Figure b is the $\tilde{C}_{k^*}(r)$ function and presents the calculation of a reconstruction kernel K_{k^*} . Figure c is the reconstruction of $S_1^{(k^*)}(r)$ and comparison with the ground-truth source distribution.

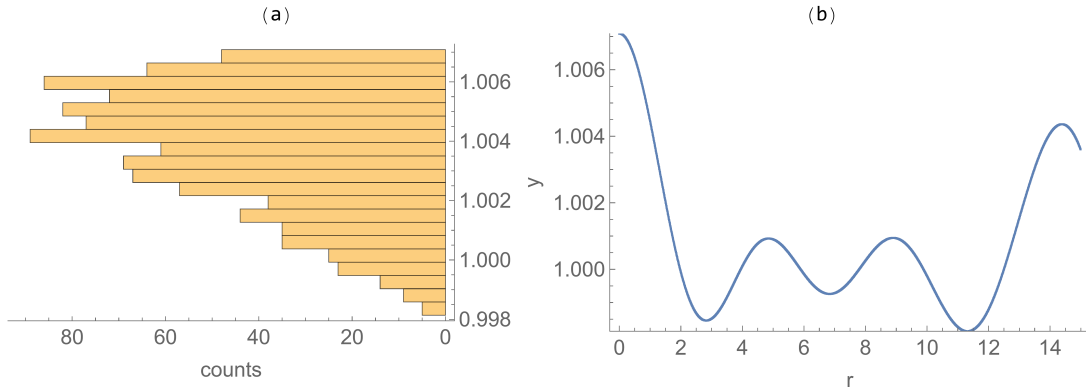


FIG. 3: Figure (a) presents the histogram of $y = \tilde{C}_{k^*}(r)$ where $k^* = 156$ MeV. Figure (b) illustrates the non-monotonic behavior of $\tilde{C}_{k^*}(r)$. This violation of bijectivity induces ambiguity in the reconstruction mapping, resulting in a bad reconstructed source distribution.

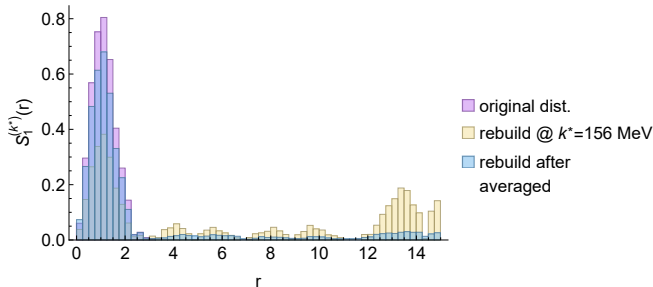


FIG. 4: A bad reconstruction example (yellow) at $k^* = 156$ MeV due to the non-monotonic behavior of $\tilde{C}_{k^*}(r)$ shown in Fig. 3. Averaging on multi-momentum reconstructions (blue) can reduce the effects of these fake peaks.

To suppress these artifacts, we average reconstructions performed at multiple momenta. This multi-momentum averaging amplifies the contribution from the true source and yields a significantly improved profile, as shown in Fig. 4.

III. RECONSTRUCT J/ψ SOURCE FROM EPOS4HQ

A. Model setup

EPOS4 is a comprehensive simulation framework for high-energy particle collisions [53–56]. It provides a fully self-consistent description of both proton-proton (pp) and nucleus-nucleus (AA) collisions by integrating four core concepts, parallel scattering (multiple partons/nucleons acting parallelly in high-energy collisions), energy conservation, factorization (separating hard processes into parton distribution functions and differential scattering cross sections), and dynamic saturation effect (screening of low transverse momentum particle production by saturation scale). The framework first models the initial particle interactions using an S-matrix approach to handle parallel scatterings. Subsequently, the collision evolution is treated through a sequence of secondary processes, beginning with core-corona separation and followed by hydrodynamic evolution to describe collective behavior, microcanonical hadronization to convert the fluid into hadrons, and finally the UrQMD hadron cascade acting as an afterburner to simulate resonant decays and hadronic rescatterings.

In pure EPOS4 framework, heavy flavor partons are

created in primary interactions. Their subsequent interactions with the simulated quark-gluon plasma are incorporated via the dedicated HQ module. This module also enables, under specific conditions, the coalescence of plasma partons with heavy-flavor partons to form heavy-flavor hadrons. The extended version, EPOS4HQ [57, 58], is endowed with the capability to describe a wide range of heavy-flavor observables from experiments and remains accessible for further studies.

To compute the correlation function in Eq. (1), we simulate 10^5 pp collisions at $\sqrt{s} = 13.6$ TeV within EPOS4HQ, which provides the spatiotemporal emission sources for protons and J/ψ . Event-wise particle samples are subjected to standard fiducial selections, protons are required to satisfy a pseudorapidity window of $-0.9 < \eta < 0.9$ and a transverse-momentum range of $0.25 < p_T < 3$ GeV/ c , while J/ψ candidates are selected with $-0.9 < \eta < 0.9$ and $p_T > 1$ GeV/ c . The $p - J/\psi$ scattering wavefunction is derived from the $N - J/\psi$ potential obtained via HAL QCD calculations [59], a non-perturbative approach extracting spatial potentials from lattice QCD [62–64]. Final-state correlations are computed using the Correlation Analysis Tool using the Schrödinger equation (CATS) [65], employing a test-particle analysis with event mixing over all simulated collisions.

B. Priori proton source

Since femtoscopic sources are local in momentum space, even high-momentum protons can still contribute to the $p - p$ correlation when their momentum directions are strongly aligned due to collective flow. While the flow effect on J/ψ is weaker, especially in pp collisions, the proton- and J/ψ - emission process is regraded as uncorrelated and particle momentum magnitude is the primary criterion for particle selection in the $p - J/\psi$ correlation analysis. However, the proton source is different in $p - p$ and $p - J/\psi$ correlations, and we can not extract proton source via $p - p$ correlation for $p - J/\psi$ pair analysis. In this simulation, the relative momentum is restricted to $0 < k^* < 400$ MeV/ c . For a pair with momenta p_1 for proton and p_2 for J/ψ , the constraint on k^* imposes a strong kinematic constraint on the opening angle θ_{12} , since $k^* = \frac{1}{2}\sqrt{p_1^2 + p_2^2 - 2p_1p_2 \cos \theta_{12}}$. When particles have large momenta, the acceptance of p_1 and p_2 ,

$$\text{Acc}(p_1, p_2) = \int_0^{400} \sin(\theta_{12}) \frac{\partial \theta_{12}}{\partial k} dk / 2, \quad (12)$$

can be small due to a narrow θ_{12} interval. Therefore, pairs with large p_1 and p_2 contribute weakly to the selected k^* region. This provides the practical basis for selecting protons within a controlled momentum window to construct the priori reference source in the present reconstruction framework.

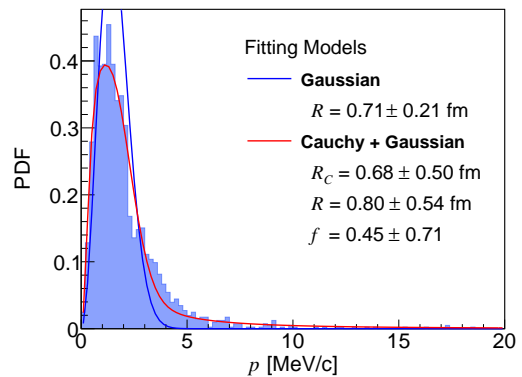


FIG. 5: The protons with momentum < 400 MeV/ c are selected as the known reference source. The spatial distribution is generated by EPOS4HQ and fitted with Gaussian distribution as well as Eq. (13), where Gaussian + Cauchy distribution performs better.

In this simulation, protons with momentum < 400 MeV/ c are selected as the known reference source. To obtain its spatial distribution, we adopt the Gaussian core + Cauchy tail [27, 28],

$$S_p(r) = f \frac{R_C}{\pi^2 (R_C^2 + r^2)^2} + (1-f) \frac{1}{\sqrt{4\pi R^2}^3} \exp\left(-\frac{r^2}{4R^2}\right), \quad (13)$$

to describe the proton source generated by EPOS4, with $R_C \simeq 0.68$ fm, $R \simeq 0.80$ fm and the mixing fraction $f \simeq 0.51$ (Fig. 5). Although this fitting introduces model dependence into our reconstruction framework, proton sources have been extensively studied in different phenomenological models and are constrained by available experimental data. The model-to-model differences are relatively small and can be incorporated as a systematic uncertainty in the present reconstruction.

C. Extracting J/ψ source

The $p - J/\psi$ correlation function and the corresponding source fits are presented in Fig. 6. Crucially, the extracted $p - J/\psi$ source exhibits significantly smaller spatial extent than the two-proton source obtained in Sec. III B, implying that J/ψ mesons are emitted from a more compact region compared to protons. This finding provides direct motivation for applying our statistical reconstruction framework to reconstruct the J/ψ emission source from EPOS4HQ simulations. A conventional fitting strategy is used as a benchmark to compare our methodology (Fig. 6). Since the resulting mixing fraction f of Gaussian + Cauchy distribution is found to be small in describing $p - J/\psi$ pair source, the pair source can be well described by a single Gaussian component. Adopting the assumption of uncorrelated emission process, we extract a single- J/ψ Gaussian radius of $R_{J/\psi} \simeq 0.37$ fm, with a single-proton Gaussian source fitted in Fig. 5.

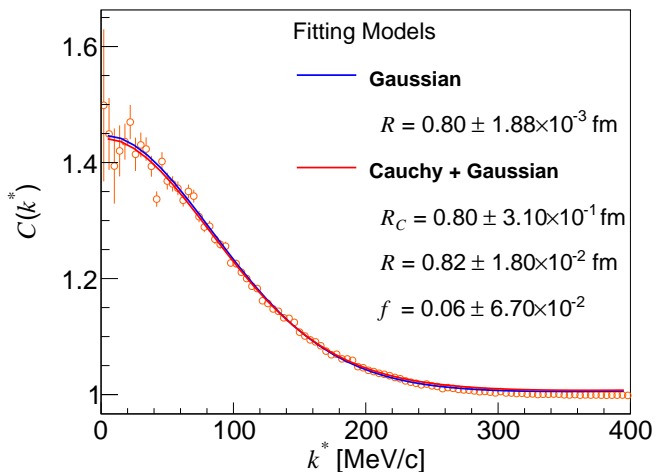


FIG. 6: The $p - J/\psi$ correlation function (orange markers) in $\sqrt{s} = 13.6$ TeV pp collisions, calculated from EPOS4HQ-simulated particle sources and HAL QCD $N - J/\psi$ potentials. Results from two candidate source model fits are also shown with a same fitting range in $p - p$ correlation. The extracted mixing fraction f is found to be very small, demonstrating that the two-particle source is well described by a single Gaussian model.

As discussed in Sec. II A, a key distinction between experiment and simulation lies in the nature of the $\tilde{C}_{k^*,i}$ observable. Experimentally measured values (Eq. (8)) are discrete, whereas those computed from simulations (Eq. (4)) are continuous. To emulate the discrete character of experimental data, we discretize the simulated continuous \tilde{C}_{k^*} value via

$$n_i^{\text{same}} = \left\lfloor \frac{\tilde{C}_{k^*} N^{\text{mixed}}(k^*)}{\mathcal{N} N_{\text{events}}^{\text{rare}}(k^*)} \right\rfloor, \quad (14)$$

where, $\lfloor x \rfloor$ denotes the floor function, rounding x down to the nearest integer. Within the test-particle method used here, the normalization factor $\mathcal{N} = 1$. The number of uncorrelated pairs $N^{\text{mixed}}(k^*)$ corresponds to the total count of $p - J/\psi$ pairs at momentum k^* in the EPOS4HQ-generated final-state phase space. $N_{\text{events}}^{\text{rare}}$ denotes the number of events containing one J/ψ . Because the J/ψ yield is rare, the number of J/ψ particles (Eq. (8)) is approximately equal to the number of events containing J/ψ in Eq. (14). Therefore, fluctuations associated with event-wise particle multiplicity are strongly suppressed. Substituting n_i^{same} back into Eq. (8) yields the discretized $\tilde{C}_{k^*,i}$, which then serves as the input for reconstructing the J/ψ emission source using the Statistical Reconstruction method.

Following the methodology in Sec. II, we analytically compute $\tilde{C}_{k^*}(r)$ over $r \in [0, 15]$ fm. The resulting two-dimensional domain of the function on the r - y plane is then discretized into 40 bins along the r -axis and coarsely binned along the y -axis. The coarse y -binning is chosen

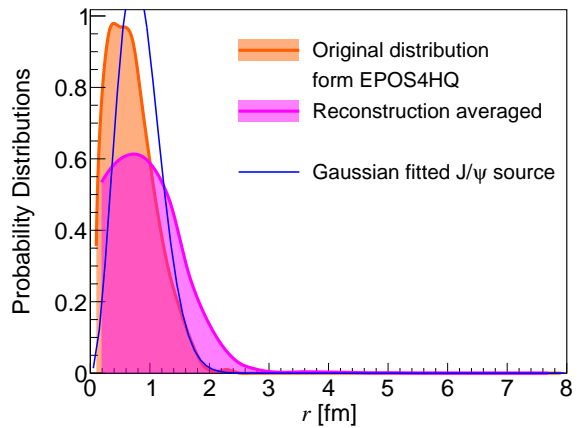


FIG. 7: Comparison between original J/ψ source and reconstruction result averaged over $k^* = 82, \dots, 238$ MeV. The Gaussian parametrizations of J/ψ source extracted from Fig. 6 are also displayed as a comparison.

to accommodate the spread of the discrete $\tilde{C}_{k^*,i}$ values and is determined by the range of the analytically computed $\tilde{C}_{k^*}(r)$.

Fig. 7 shows the reconstructed J/ψ emission source averaged over the momentum range $k^* = 82, \dots, 238$ MeV. While the reconstruction exhibits a broader spatial distribution and a more pronounced tail compared to the original EPOS4HQ-simulated J/ψ source, it preserves key characteristics such as the most probable radius and the overall compactness. Notably, the most probable radius agrees better with the original simulation than that obtained from a simple Gaussian fit to the J/ψ source.

In line with our initial conjecture in Sec. I, the reconstructed J/ψ source is more compact than the proton source. Using the fitted proton source together with the reconstructed J/ψ source, we compute the corresponding correlation function (magenta curve in Fig. 8). This reconstructed correlation is weaker than the one derived directly from the EPOS4HQ simulations. The discrepancy that originates from the broader spread and enhanced tail structure present in the reconstructed source (Fig. 7).

The systematic uncertainty of the Statistical Reconstruction method is estimated via

$$\delta_{\text{sys.}} \sim \frac{C_{\text{recon.}}(k^*) - 1}{C(k^*) - 1}, \quad (15)$$

where $C(k^*)$ denotes the $p - J/\psi$ correlation function computed directly from EPOS4HQ simulation, and $C_{\text{recon.}}(k^*)$ is the result obtained from our reconstruction. This yields a systematic uncertainty of approximately 13% for this J/ψ source reconstruction. One contributor to this systematic error is the discretization of the \tilde{C}_{k^*} values, as well as the simple Gaussian parameterization used for the proton source.

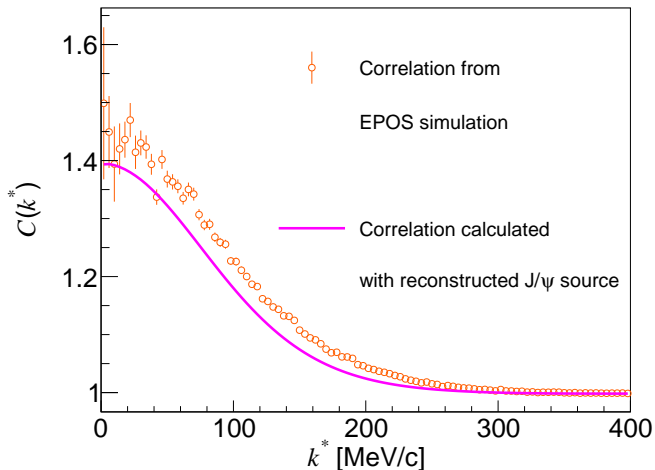


FIG. 8: Comparison of the $p - J/\psi$ correlation function obtained from direct EPOS4HQ simulation with the result reconstructed using the Statistical Reconstruction method. The shaded region indicates the momentum interval employed in the multi-momentum averaging. This comparison is used to estimate the systematic uncertainty of the method, yielding an uncertainty of approximately 13% in present analysis.

IV. SUMMARY

The present study presents a Statistical Reconstruction method for reconstructing the single-particle emission source of rare particles without the Gaussian parametrization. The method is based on the particle-particle distribution of the single-particle-conditioned correlation kernel, which is easier to be experimentally accessible when at most one rare particle is produced per collision event and suppress the fluctuations associated with particle multiplicity. This key property enables a direct statistical reconstruction of the single-particle source, rather than an indirect inference from effective two-particle sources.

Leveraging a well-characterized reference-particle source and a constrained interaction potential, the conditioned kernel function, $\tilde{C}_{k^*}(r)$ is computed analytically. Its radial derivative defines a momentum-dependent reconstruction kernel K_{k^*} , through which the spatial extent of the target particle source is obtained from the measured kernel distribution. To suppress reconstruction

artifacts arising from non-monotonic $\tilde{C}_{k^*}(r)$ behavior as increasing r , a multi-momentum averaging procedure is employed as a stabilization strategy.

We conduct two validation studies, Gaussian source reconstruction and EPOS4HQ-simulated J/ψ source reconstruction, to evaluate the method and quantify its systematic uncertainties. In the Gaussian case, Monte Carlo sampling is used to generate the spatial distribution and compute the \tilde{C}_{k^*} distribution, with multi-momentum averaging yielding an accurate reconstruction. For the more complex EPOS4HQ validation, we use $p - J/\psi$ correlations to reconstruct J/ψ source. The proton source, extracted by fitting spatial distribution of protons with momentum < 400 MeV simulated in EPOS4HQ, serves as the known single-particle source input. Meanwhile, the HAL QCD-derived $N - J/\psi$ potentials are used to calculate the $p - J/\psi$ correlation and the conditioned kernel \tilde{C}_{k^*} . Applying multi-momentum averaging, the reconstructed J/ψ source preserves key characteristics, including the most probable radius and intrinsic compactness. A comparison between the directly simulated and reconstructed $p - J/\psi$ correlation functions reveals a systematic uncertainty of approximately 13% for J/ψ source reconstruction.

In summary, the proposed Statistical Reconstruction method enables reconstruction of rare-particle emission sources without assumptions on the shape of one-particle emission source. This approach could provide quantitative constraints on rare-particle source characteristics and offer deeper insights into the intermediate processes of both pp and heavy-ion collisions. The methodology can further serve as a useful tool for future femtoscopy analysis.

ACKNOWLEDGMENTS

This work was supported in part by the National Natural Science Foundation of China under contract Nos. 12275054, 12147101, 12061141008, 12347106, 12422509, 12375121, and 12547102, National Key R&D Program of China under Grant No. 2024YFA1610802 and 2018YFE0104600, the Guangdong Major Project of Basic and Applied Basic Research No. 2020B0301030008, Shanghai Pilot Program for Basic Research - Fudan University 21TQ1400100(22TQ006) and the STCSM under Grant No. 23590780100.

-
- [1] R. Hanbury Brown and R. Q. Twiss, *Nature* **178**, 1046 (1956).
 - [2] G. Goldhaber, S. Goldhaber, W. Lee, and A. Pais, *Phys. Rev.* **120**, 300 (1960).
 - [3] G. Kopylov, *Phys. Lett. B* **50**, 472 (1974).
 - [4] W. A. Zajc, J. A. Bistirlich, R. R. Bossingham, *et al.*, *Phys. Rev. C* **29**, 2173 (1984).
 - [5] D. H. Boal, C. K. Gelbke, and B. K. Jennings, *Rev. Mod. Phys.* **62**, 553 (1990).
 - [6] W. Bauer, C. K. Gelbke, and S. Pratt, *Ann. Rev. Nucl. Part. Sci.* **42**, 77 (1992).
 - [7] M. A. Lisa, S. Pratt, R. Soltz, and U. Wiedemann, *Ann. Rev. Nucl. Part. Sci.* **55**, 357 (2005), [arXiv:nuclex/0505014](https://arxiv.org/abs/nuclex/0505014).

- [8] U. Heinz and B. V. Jacak, *Annu. Rev. Nucl. Part. Sci.* **49**, 529 (1999), [arXiv:nucl-th/9902020](#).
- [9] U. A. Wiedemann and U. Heinz, *Phys. Rep.* **319**, 145 (1999).
- [10] J. H. Chen, X. Dong, H. Z. Huang, *et al.*, *Nucl. Sci. Tech.* **35**, 214 (2024).
- [11] Q. Y. Shou, Y. G. Ma, S. Zhang, *et al.*, *Nucl. Sci. Tech.* **35**, 219 (2024).
- [12] P. Lu, R. Kavak, A. Dubla, S. Masciocchi, and I. Seyluzhenkov, *Nucl. Sci. Tech.* **36**, 142 (2025).
- [13] R. Q. Wang, X. L. Hou, Y. H. Li, J. Song, and F. L. Shao, *Nucl. Sci. Tech.* **36**, 185 (2025).
- [14] N. Yu, Z. M. Zhang, H. G. Xu, and M. X. Song, *Nucl. Sci. Tech.* **36**, 65 (2025).
- [15] W. J. Dong, X. Z. Yu, S. Y. Ping, *et al.*, *Nucl. Sci. Tech.* **35**, 120 (2024).
- [16] R. Lednicky and V. L. Lyuboshits, *Yad. Fiz. (sov. J. Nucl. Phys.)* **35**, 1316 (770) (1981).
- [17] S. Pratt, *Phys. Rev. D* **33**, 1314 (1986).
- [18] M. Bowler, *Phys. Lett. B* **270**, 69 (1991).
- [19] R. Lednicky and V. L. Lyuboshitz, *Acta Phys. Hung. New Ser. Heavy Ion Phys.* **3**, 93 (1996).
- [20] R. Lednicky, in *Int. Workshop Phys. Quark Gluon Plasma* (2001).
- [21] R. Lednicky, in *Multiparticle Dyn.* (WORLD SCIENTIFIC, Alushta, Crimea, Ukraine, 2003) pp. 21–26, [arXiv:nucl-th/0212089](#).
- [22] Y. B. Wei, Y. G. Ma, W. Q. Shen, *et al.*, *Phys. Lett. B* **586**, 225 (2004).
- [23] Y. G. Ma, G. H. Liu, X. Z. Cai, *et al.*, *Phys. Rev. C* **85**, 024618 (2012).
- [24] Y. G. Ma, D. Q. Fang, X. Y. Sun, *et al.*, *Phys. Lett. B* **743**, 306 (2015).
- [25] S. E. Koonin, *Phys. Lett. B* **70**, 43 (1977).
- [26] J. He, S. Zhang, Y.-G. Ma, J. Chen, and C. Zhong, *Eur. Phys. J. A* **56**, 52 (2020), [arXiv:2002.06058 \[nucl-th\]](#).
- [27] ALICE Collaboration (ALICE), *Phys. Lett. B* **811**, 135849 (2020), [arXiv:2004.08018 \[nucl-ex\]](#).
- [28] ALICE Collaboration (ALICE), *Eur. Phys. J. C* **85**, 198 (2025), [arXiv:2311.14527 \[hep-ph\]](#).
- [29] J. Xu, Z. Qin, R. Zou, D. Si, S. Xiao, B. Tian, Y. Wang, and Z. Xiao, *Chin. Phys. Lett.* **42**, 31401 (2025), [arXiv:2411.08718 \[nucl-th\]](#).
- [30] A.-S. Xiong, Q.-W. Yuan, M.-Z. Liu, F.-S. Yu, Z.-W. Liu, and L.-S. Geng, *Solving the inverse source problem in femtoscopy with a toy model* (2025), [arXiv:2512.06904 \[hep-ph\]](#).
- [31] L. Wang and J. Zhao, *Learning hadron emitting sources with deep neural networks* (2025), [arXiv:2411.16343 \[nucl-th\]](#).
- [32] B.-S. Xi, J.-H. Chen, L. Ma, Y.-G. Ma, and T.-T. Wang, *Nucl. Sci. Tech.* **36**, 228 (2025).
- [33] Y. Wang, F. Guan, Q. Wu, *et al.*, *Phys. Lett. B* **825**, 136856 (2022), [arXiv:2112.02210 \[nucl-ex\]](#).
- [34] T.-T. Wang, *Phys. Rev. C* **107**, 014911 (2023), [arXiv:2301.02846 \[hep-ph\]](#).
- [35] F.-H. Qiao, X.-G. Deng, and Y.-G. Ma, *Phys. Lett. B* **850**, 138535 (2024), [arXiv:2403.04341 \[nucl-th\]](#).
- [36] T.-T. Wang, Y.-G. Ma, and S. Zhang, *Phys. Rev. C* **109**, 024912 (2024).
- [37] D.-F. Wang, M.-Y. Chen, Y.-G. Ma, Q.-Y. Shou, S. Zhang, and L. Zheng, *Nucl. Sci. Tech.* **36**, 154 (2025), [arXiv:2501.15776 \[nucl-th\]](#).
- [38] Y. G. Ma, Y. B. Wei, W. Q. Shen, *et al.*, *Phys. Rev. C* **73**, 014604 (2006), [arXiv:nucl-th/0601078](#).
- [39] STAR Collaboration (STAR), *Nature* **527**, 345 (2015), [arXiv:1507.07158 \[nucl-ex\]](#).
- [40] J. Haidenbauer, *Nucl. Phys. A* **981**, 1 (2019), [arXiv:1808.05049 \[hep-ph\]](#).
- [41] L. Fabbietti, V. M. Sarti, and O. V. Doce, *Ann. Rev. Nucl. Part. Sci.* **71**, 377 (2021), [arXiv:2012.09806 \[nucl-ex\]](#).
- [42] ALICE Collaboration (ALICE), *Phys. Lett. B* **844**, 137223 (2022), [arXiv:2204.10258 \[nucl-ex\]](#).
- [43] ALICE Collaboration (ALICE), *Phys. Rev. Lett.* **127**, 172301 (2021), [arXiv:2105.05578 \[nucl-ex\]](#).
- [44] D. Si, S. Xiao, Z. Qin, *et al.*, *Phys. Rev. Lett.* **134**, 222301 (2025), [arXiv:2501.09576 \[nucl-ex\]](#).
- [45] L. Adamczyk *et al.* (STAR), *Phys. Rev. Lett.* **114**, 022301 (2015).
- [46] Y. Kamiya, T. Hyodo, K. Morita, A. Ohnishi, and W. Weise, *Phys. Rev. Lett.* **124**, 132501 (2020), [arXiv:1911.01041 \[nucl-th\]](#).
- [47] ALICE Collaboration (ALICE), *Phys. Lett. B* **845**, 138145 (2023), [arXiv:2305.19093 \[nucl-ex\]](#).
- [48] ALICE Collaboration (ALICE), *Eur. Phys. J. A* **61**, 194 (2025), [arXiv:2502.20200 \[nucl-ex\]](#).
- [49] ALICE Collaboration (ALICE), *Nature* **648**, 306 (2025), [arXiv:2504.02393 \[nucl-ex\]](#).
- [50] K. J. Sun, *Nucl. Sci. Tech.* **37**, 64 (2026).
- [51] M.-Z. Liu, Y.-W. Pan, Z.-W. Liu, T.-W. Wu, J.-X. Lu, and L.-S. Geng, *Phys. Rept.* **1108**, 2368 (2024), [arXiv:2404.06399 \[hep-ph\]](#).
- [52] J. H. Chen, F. K. Guo, J. J. Wu, B. S. Zou, Y. G. Ma, C. P. Shen, and Q. Y. Shou, *Nucl. Sci. Tech.* **36**, 55 (2025).
- [53] K. Werner and B. Guiot, *Phys. Rev. C* **108**, 034904 (2023).
- [54] K. Werner, *Phys. Rev. C* **108**, 064903 (2023), [arXiv:2301.12517](#).
- [55] K. Werner, *Phys. Rev. C* **109**, 014910 (2024).
- [56] K. Werner, *Phys. Rev. C* **109**, 034918 (2024).
- [57] J. Zhao, J. Aichelin, P. B. Gossiaux, and K. Werner, *Phys. Rev. D* **109**, 054011 (2024).
- [58] J. Zhao, J. Aichelin, P. B. Gossiaux, V. Ozvenchuk, and K. Werner, *Phys. Rev. C* **110**, 024909 (2024).
- [59] Y. Lyu, T. Doi, T. Hatsuda, and T. Sugiura, *Phys. Lett. B* **860**, 139178 (2024), [arXiv:2410.22755 \[hep-lat\]](#).
- [60] ALICE Collaboration (ALICE), *Nature* **588**, 232 (2021), [arXiv:2005.11495 \[nucl-ex\]](#).
- [61] ALICE Collaboration (ALICE), *Phys. Rev. Lett.* **124**, 092301 (2020), [arXiv:1905.13470 \[nucl-ex\]](#).
- [62] N. Ishii, S. Aoki, and T. Hatsuda, *Phys. Rev. Lett.* **99**, 022001 (2007), [arXiv:nucl-th/0611096](#).
- [63] N. Ishii, S. Aoki, T. Doi, T. Hatsuda, Y. Ikeda, T. Inoue, K. Murano, H. Nemura, and K. Sasaki (HAL QCD), *Phys. Lett. B* **712**, 437 (2012), [arXiv:1203.3642 \[hep-lat\]](#).
- [64] S. Aoki and T. Doi, *Front. in Phys.* **8**, 307 (2020), [arXiv:2003.10730 \[hep-lat\]](#).
- [65] D. L. Mihaylov, V. Mantovani Sarti, O. W. Arnold, L. Fabbietti, B. Hohlweger, and A. M. Mathis, *Eur. Phys. J. C* **78**, 394 (2018), [arXiv:1802.08481 \[hep-ph\]](#).